

## Development of an Immune-Pathology Informed Radiomics Model for Non-Small Cell Lung Cancer

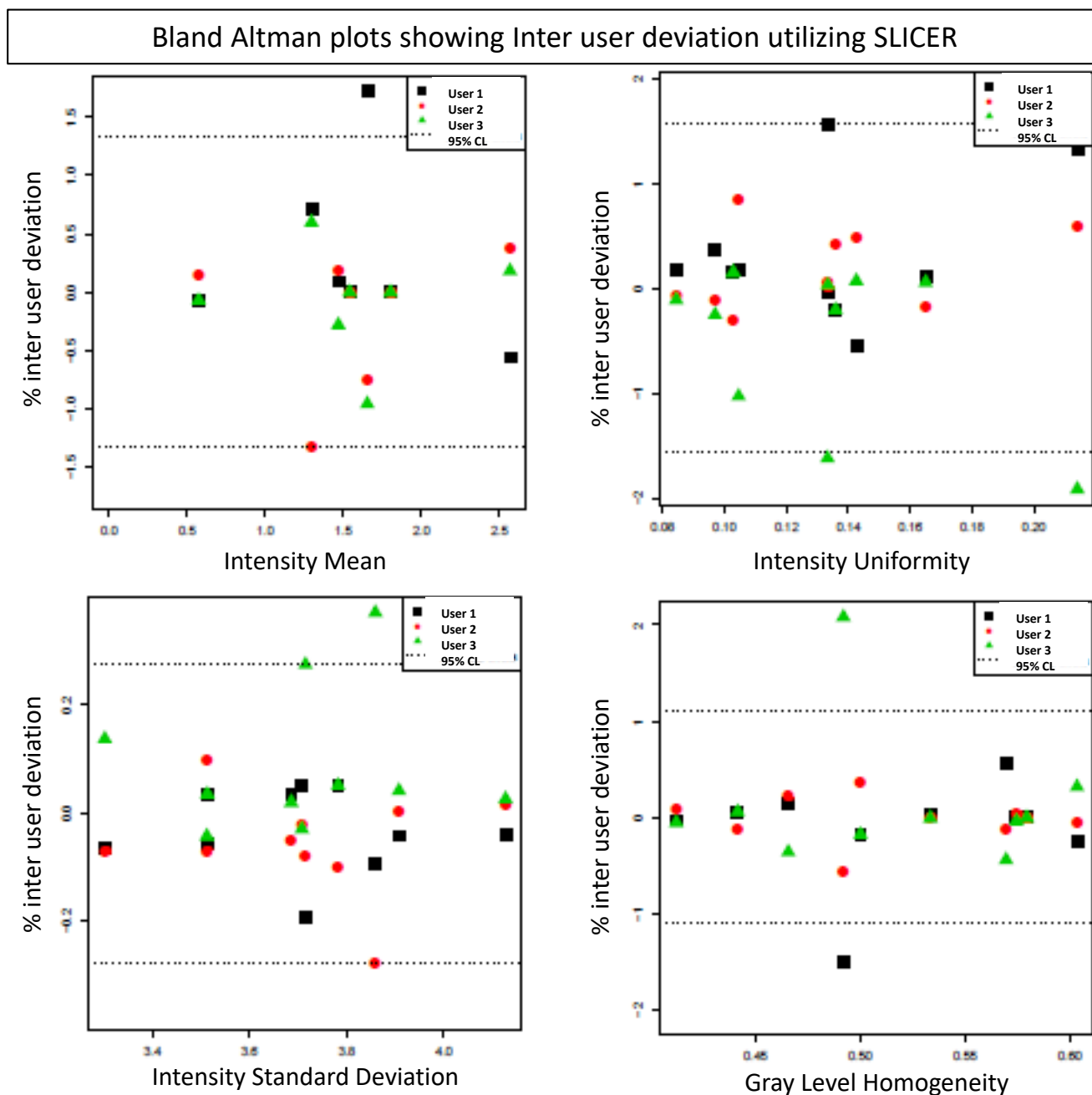
Supplemental Items

### **Authors:**

Chad Tang  
Brian Hobbs  
Ahmed Amer  
Xiao Li  
Carmen Behrens  
Jaime Rodriguez Canales  
Edwin Parra Cuentas  
Pamela Villalobos  
David Fried  
Joe Y. Chang  
David S. Hong  
James W. Welsh  
Boris Sepesi  
Laurence Court  
Ignacio I. Wistuba  
Eugene J. Koay

	SLICER	MIMvista
Voxel intensity metrics	Mean*	± 1.5%
	Kurtosis	± 7.4%
	Skewness	± 10.6%
	Entropy	± 0.9%
	Std deviation*	± 0.4%
	Uniformity*	± 2.4%
Gray level co-occurrence	Contrast	± 3.1%
	Dissimilarity	± 5.2%
	Energy	± 6.2%
	Entropy	± 1.7%
	Homogeneity	± 0.6%
	Modified Homogeneity	± 0.6%

\*indicates features utilized in the immune pathology informed model (IPIM)



**Supplementary Fig. S1.** Inter-user deviation comparing radiomics features created from contours from 3 different radiation oncologists in 2 different contouring programs (SLICER and MIMvista). Representative Bland Altman plots are shown for 4 highly reproducible features (defined as



**Supplementary Fig. S2.** Representative segmentations of lung tumors.

**Supplemental Table S1.** Multivariate associations with survival assessing pathology status

Characteristic	Training Set (n=114)			Validation Set (n=176)		
	HR	95% CI	P Value	HR	95% CI	P Value
Lesion size (per cm)	1.19	1.03-1.36	0.02	1.04	0.92-1.18	0.53
N1/N2 (vs. N0)	1.16	0.67-2.02	0.60	4.92	2.70-8.96	<0.01
Adjuvant therapy (vs. none)	0.84	0.47-1.52	0.57	0.58	0.30-1.12	0.10
Age at surgery (per year)	1.04	1.01-1.07	0.02	1.03	1.00-1.07	0.04
Squamous histology	1.03	0.60-1.77	0.91	1.50	0.92-2.45	0.11
Current smoker (vs. former and never smoker)	1.14	0.67-1.95	0.62	1.24	0.74-2.09	0.41
Radiomics cluster (REF: CD3 <sup>lo</sup> PDL1 <sup>hi</sup> )						
CD3 <sup>hi</sup> PDL1 <sup>hi</sup>	1.06	0.44-2.56	0.89	0.37	0.20-0.69	<0.01
CD3 <sup>hi</sup> PDL1 <sup>lo</sup>	0.31	0.10-0.95	0.04	0.14	0.03-0.57	<0.01
CD3 <sup>lo</sup> PDL1 <sup>lo</sup>	0.87	0.50-1.52	0.62	1.24	0.74-2.09	0.01

Abbreviations: 95% CI, 95% confidence interval; HR, hazard ratio

Histology groupings are as follows, CD3<sup>lo</sup>PDL1<sup>hi</sup>: CD3 low and PDL1 high, CD3<sup>hi</sup>PDL1<sup>hi</sup>: CD3 high and PDL1 high, CD3<sup>hi</sup>PDL1<sup>lo</sup>: CD3 high and PDL1 low, CD3<sup>lo</sup>PDL1<sup>lo</sup>: CD3 low and PDL1 low.

**Supplemental Table S2.** Sensitivity analysis, multivariate associations with survival in patients with negative resection margins

<b>Characteristic</b>	<b>Training Set (n=107)</b>			<b>Validation Set (n=167)</b>			<b>Validation Set (Stage 1 only; n=107)</b>		
	HR	95% CI	<i>P</i> Value	HR	95% CI	<i>P</i> Value	HR	95% CI	<i>P</i> Value
Lesion size (per cm)	1.18	1.02-1.36	0.03	0.96	0.81-1.12	0.59	1.11	0.73-1.69	0.62
N1/N2 (vs. N0)	1.61	0.86-3.01	0.30	3.92	2.09-7.36	<0.01	—	—	—
Adjuvant therapy (vs. none)	0.64	0.34-1.19	0.16	0.76	0.40-1.47	0.42	0.55	0.06-4.68	0.58
Age at surgery (per year)	1.05	1.01-1.08	0.02	1.01	0.98-1.04	0.44	1.06	1.00-1.12	0.04
Squamous histology	0.81	0.47-1.41	0.81	1.70	1.01-2.88	0.047	1.75	0.80-3.87	0.16
Current smoker (vs. former and never smoker)	1.26	0.71-2.24	0.43	1.06	0.61-1.83	0.84	0.76	0.31-1.82	0.57
Radiomics cluster (REF: Cluster D)									
Cluster A	1.59	0.44-5.81	0.48	1.58	0.71-3.52	0.26	2.77	1.07-7.20	0.04
Cluster B	3.71	1.07-12.80	0.04	1.52	0.69-3.38	0.30	1.00	0.23-4.33	>0.99
Cluster C	2.79	0.78-9.92	0.11	2.80	1.22-6.43	0.02	4.94	1.88-13.00	<0.01

Abbreviations: 95% CI, 95% confidence interval; HR, hazard ratio

**Supplemental Table S3: Voxel intensity metrics**

Feature	Feature Algorithm	Ref	Preprocessing	Preprocessing Parameters
Mean	$\sum_{i=1}^{Ng} i * h(i)$	3,4,5	Threshold_Image_Mask Log_Filter	ThresholdLow=900; ThresholdHigh=8000; ErosionDist=0; Size=15; Sigma=1; FillROIOutOn=1; FillROIOutValue=5000;
Kurtosis	$\frac{\sum_{i=1}^{Ng} (i - \sum_{i=1}^{Ng} i * h(i))^4 * h(i)}{(\sum_{i=1}^{Ng} (i - \sum_{i=1}^{Ng} i * h(i))^2 * h(i))^2}$	3,4,5	Threshold_Image_Mask	ThresholdLow=900; ThresholdHigh=8000; ErosionDist=0;
Skewness	$\frac{\sum_{i=1}^{Ng} (i - \sum_{i=1}^{Ng} i * h(i))^3 * h(i)}{(\sum_{i=1}^{Ng} (i - \sum_{i=1}^{Ng} i * h(i))^2 * h(i))^{3/2}}$	3,4,5	BitDepthRescale_Range	RangeMin=0; RangeMax=4096; RangeFix=1; BitDepth=8;
Entropy	$-\sum_{i=1}^{Ng} h(i) * \log(h(i))$	3,4,5	Threshold_Image_Mask	ThresholdLow=900; ThresholdHigh=8000; ErosionDist=0;
Standard Deviation	$\sqrt{\sum_{i=1}^{Ng} (i - \sum_{i=1}^{Ng} i * h(i))^2 * h(i)}$	3,4,5		
Uniformity	$\sum_{i=1}^{Ng} h(i)^2$	4,5		

Ng is the number of grey levels, h(i) is the probability of intensity i. All labels and parameter nomenclature are in reference to that utilized in IBEX.

**Supplemental Table S4:** Gray level co-occurrence metrics

Feature	Feature Algorithm	Ref	Preprocessing	Preprocessing Parameters
Contrast	$\sum_{n=0}^{Ng-1} n^2 \left\{ \sum_{i=1}^{Ng} \sum_{j=1}^{Ng} p(i,j) \mid  i-j  = n \right\}$	1,2	Threshold_Image_Mask	ThresholdLow=900; ThresholdHigh=8000; ErosionDist=0;
Dissimilarity	$\sum_{i=1}^{Ng} \sum_{j=1}^{Ng}  i-j  * p(i,j)$	1,2	BitDepthRescale_Range	RangeMin=0; RangeMax=4096; RangeFix=1; BitDepth=8;
Energy	$\sum_{i=1}^{Ng} \sum_{j=1}^{Ng} p(i,j)^2$	1,2		
Entropy	$-\sum_{i=1}^{Ng} \sum_{j=1}^{Ng} p(i,j) * \log(p(i,j))$	1,2		
Homogeneity	$\sum_{i=1}^{Ng} \sum_{j=1}^{Ng} \frac{1}{1 +  i-j } * p(i,j)$	1,2		
Modified Homogeneity	$\sum_{i=1}^{Ng} \sum_{j=1}^{Ng} \frac{1}{1 + (i-j)^2} * p(i,j)$	2		

Ng is the number of grey levels, p(i,j) is the (i,j)th element in the Grey Level Cooccurrence Matrix (GLCM) respectively. All labels and parameter nomenclature are in reference to that utilized in IBEX.

## References:

1. L. Soh and C. Tsatsoulis. Texture analysis of sar sea ice imagery using gray level co-occurrences matrices. IEEE Trans. on Geoscience and Remote Sensing, 37(2):780-795, 1999.
2. Hugo J. W, Sara Cavalho, et al. Decoding tumour phenotype by noninvasive imaging using a quantitative radiomics approach. Nat. Commun. 2014; 5: 4006.
3. Basu S. Developing Predictive Models for Lung Tumor Analysis. University of South Florida; 2012.
4. Cunliffe AR, Armato SG, 3rd, Fei XM, et al. Lung texture in serial thoracic CT scans: registration-based methods to compare anatomically matched regions. Med Phys. 2013;40(6):061906.
5. Fried DV, Tucker, S. L., Zhou, S., Liao, Z., Mawlawi, O., Ibbott, G., Court, L. E. . Prognostic value and reproducibility of pretreatment CT texture features in stage III Non-Small-Cell lung cancer Int J Radiation Oncol Biol Phys. 2014.